

DARK SOLITONS FOR AN EXTENDED QUINTIC NONLINEAR  
SCHRÖDINGER EQUATION: APPLICATION TO WATER WAVES AT  
 $kh = 1.363$

F. TSITOURA<sup>1</sup>, T. P. HORIKIS<sup>2</sup>, D. J. FRANTZESKAKIS<sup>1,\*</sup>

<sup>1</sup>Department of Physics, University of Athens, Panepistimiopolis, Zografos, Athens 15784, Greece

\*Corresponding author's Email: [dfrantz@phys.uoa.gr](mailto:dfrantz@phys.uoa.gr)

<sup>2</sup>Department of Mathematics, University of Ioannina, Ioannina 45110, Greece

*Compiled February 13, 2019*

*Abstract.* We study the existence, formation and dynamics of gray solitons for an extended quintic nonlinear Schrödinger (NLS) equation. The considered model finds applications to water waves, when the characteristic parameter  $kh$  – where  $k$  is the wavenumber and  $h$  is the undistorted water's depth – takes the critical value  $kh = 1.363$ . It is shown that this model admits approximate dark soliton solutions emerging from an effective Korteweg-de Vries equation and that two types of gray solitons exist: fast and slow, with the latter being almost stationary objects. Analytical results are corroborated by direct numerical simulations.

*Key words:* Dark solitons, water waves, Korteweg-de Vries equation, extended quintic nonlinear Schrödinger equation, reductive perturbation method.

*PACS:* 05.45.Yv, 47.35.Fg, 02.30.Jr, 02.30.Mv

## 1. INTRODUCTION

It is well known that the one-dimensional (1D) defocusing nonlinear Schrödinger (NLS) equation governing the complex field  $u = u(x, t)$ , namely:

$$iu_t + p_0 u_{xx} - q_0 |u|^2 u = 0, \quad (1)$$

with  $p_0, q_0 \in \mathbb{R}_+$ , supplemented with nonvanishing boundary conditions at infinity, i.e.,  $|u| = u_0 \in \mathbb{R}$  for  $|x| \rightarrow \infty$ , possesses dark soliton solutions [1]. These structures are localized density depressions (“notches”) off of a stable continuous-wave (cw) background, associated with a phase jump at the density minimum, and are called “black” or “gray” depending on whether the density minimum is zero or non-zero, respectively. There exists a vast amount of theoretical work and experimental observations of dark solitons in optical systems featuring a defocusing nonlinearity [2] and Bose-Einstein condensates (BECs) with repulsive interatomic interactions [3–5] (see also the review [6]). Nevertheless, dark solitons also arise in a variety of other physical systems, such as discrete mechanical [7] and electrical [8] lattices, magnetic

films [9], complex plasmas [10], nematic liquid crystals [11], and others.

Dark solitons are also known to exist in other versions of the NLS equation, such as the one featuring competing cubic and quintic nonlinearities [12–15]; the relevant, so-called cubic-quintic NLS (cqNLS) model is of the form:

$$iu_t + pu_{xx} - q|u|^2u + r|u|^4u = 0, \quad (2)$$

with  $p, q, r \in \mathbb{R}_+$ . This model appears naturally in the context of nonlinear optics as an approximation of a saturable defocusing nonlinearity, through its Taylor expansion up to second order in the normalized intensity  $I = |u|^2$  [2]. Furthermore, Eq. (2) also finds applications in the context of atomic BECs, with the quintic term accounting for three-body interactions, provided that losses due to such interactions may be neglected – see, e.g., Refs. [16, 17] and rigorous analysis in Ref. [18]. Additionally, in the same context of atomic BECs, the quintic term may appear generically in the case where weak deviations from one-dimensionality are taken into regard [19] (see also Ref. [20] for the case of attractive BECs). It is also worth mentioning that a defocusing, purely quintic NLS model [i.e.,  $q = 0$  and  $r < 0$  in Eq. (2)] has also been used as a mean-field model describing strongly interacting 1D Bose gases and, particularly, the so-called Tonks-Girardeau gas of impenetrable bosons [21]; for such systems, dark solitons of the defocusing quintic NLS were found in an exact analytical form [22] and their dynamics in the trap was also investigated [23].

More recently, there has been an interest in dark solitons in the context of surface gravity water waves: indeed, black [24] and gray [25] solitons were observed on the surface of water in two seminal experiments performed in water wave tanks. Key to this achievement was the conduction of the experiments in the regime where  $kh < 1.363$  (here,  $k$  is the wavenumber and  $h$  is the undistorted water depth): indeed, in this regime, the pertinent NLS equation governing weakly nonlinear water waves [26], becomes of the *defocusing* type. In this case, the cw solution of the NLS model is *not* subject to the Benjamin-Feir instability (also known as “modulational instability” (MI) [27]) and can, thus, support nonlinear excitations, such as the black and gray solitons observed in the experiments. Notice that in the opposite case, where  $kh > 1.363$ , the NLS equation is of the *focusing* type, its cw solution is modulationally unstable, and this gives rise (instead of dark solitons) to other localized structures observed in experiments, such as bright solitons [28] and rogue waves [29] (see also the recent review [30]).

According to the above, it becomes clear that the value of  $kh$  is of paramount importance, as it controls both the nature of the underlying NLS model (focusing/defocusing) and the type of its soliton solutions. At the critical value,  $kh = 1.363$ , the coefficient of the cubic nonlinear term of the NLS vanishes and, at this order of approximation, the model equation becomes a linear Schrödinger equation for a free particle, featuring only dispersion. Then, a natural question is which types of local-

ized water wave structures can be supported at  $kh = 1.363$ . Obviously, to address this problem, one should resort and analyze a model resulting at a higher-order of approximation, thus incorporating higher-order corrections. Several such models have been derived and studied in the literature [31–36]. All these models, are in fact special cases of the following generic equation:

$$iu_t + r_1 u_{xx} + r_2 |u|^2 u + r_3 |u|^4 u + i [r_4 |u|^2 u_x + r_5 (|u|^2)_x u] = 0, \quad (3)$$

with coefficients  $r_i \in \mathbb{R}$  ( $i \in \{1, 2, \dots, 5\}$ ), which has the following property. Equation (3) is uniformly valid, in the sense that it reduces to the classical NLS model in the limit  $r_i \rightarrow 0$  for  $i \geq 3$ , and is valid in the case under consideration, i.e., at the critical value  $kh = 1.363$ , where the coefficient of the cubic nonlinear term,  $|u|^2 u$ , is  $r_2 = 0$ . It is important to note that, as shown in Ref. [37], Eq. (3) can formally be derived from any dispersive nonlinear system via the derivative expansion method [38]. Furthermore, apart from the context of water waves, such an extended quintic NLS equation [see Eq. (3) for  $r_2 = 0$ ] finds still another physical application, as a model for wave propagation in a discrete nonlinear transmission line [39].

Motivated by the above results, our aim is to study a variant of Eq. (3) for  $r_2 = 0$ , namely an extended quintic NLS model, and show that it supports robust gray solitons – provided that the model under consideration possesses a modulationally stable cw. In fact, we will analyze, as a particular example, the model proposed by Johnson [31], which – according to the specific values of the coefficients of the model – indeed supports such a stable cw. Our methodology and main results, as well as the organization of the presentation, are described as follows. In Section 2, we present the model and reduce it to a form similar to that of Eq. (3); differences of the relevant equation with that studied in Refs. [32–34, 36], are also discussed. Then, the model under consideration is asymptotically reduced to a Korteweg-de Vries (KdV) equation via the reductive perturbation method [38]. The KdV soliton is then used to find approximate gray soliton solutions. We show that there exist two types of such solitons, slow and fast ones. The former feature a supersonic behavior – and, thus, are not physically relevant. The latter, which are particular to the case of the extended quintic NLS model under consideration, features a rapid velocity thus suggesting that stationary objects may not occur in these conditions. In Section 3, we present results of numerical simulations, which corroborate our analytical predictions. Finally, in Section 4, we summarize our conclusions.

## 2. THE MODEL AND ITS ANALYTICAL CONSIDERATION

### 2.1. THE EXTENDED QUINTIC NLS MODEL AND ITS CW SOLUTION

We start by presenting the model under consideration, derived by Johnson [31]:

$$iu_t - \alpha_1 u_{xx} - \alpha_2 |u|^2 u + \alpha_3 |u|^4 u + i [\alpha_4 |u|^2 u_x - \alpha_5 (|u|^2)_x u] - \alpha_6 u \psi_t, \quad \psi_x = |u|^2. \quad (4)$$

Here,  $u(x, t)$  is the complex amplitude of the gravity wave, and the coefficients  $\alpha_i \in \mathbb{R}_+$  ( $i \in \{1, 2, \dots, 6\}$ ). For  $kh = 1.363$ , the coefficient of the cubic term  $|u|^2 u$  becomes  $\alpha_2 = 0$ . In this case, introducing the transformations  $x \rightarrow \sqrt{\alpha_3/2\alpha_1}x$ ,  $t \rightarrow \alpha_3 t$ , and  $\psi \rightarrow \sqrt{2\alpha_1/\alpha_3}\psi$ , we cast our model in the following form:

$$iu_t - \frac{1}{2}u_{xx} + |u|^4 u + i [\beta |u|^2 u_x - \gamma (|u|^2)_x u] - \delta u \psi_t = 0, \quad \psi_x = |u|^2, \quad (5)$$

where the coefficients in Eq. (5) are given by:

$$\beta = \frac{\alpha_4}{\sqrt{2\alpha_1\alpha_3}}, \quad \gamma = \frac{\alpha_5}{\sqrt{2\alpha_1\alpha_3}}, \quad \delta = \alpha_6 \sqrt{\frac{2\alpha_1}{\alpha_3}}, \quad (6)$$

and are all positive real numbers.

Next, employing the transformation:

$$u(x, t) = v(x, t) \exp[-i\delta\psi(x, t)], \quad (7)$$

we can reduce Eq. (5) to the more convenient local form:

$$iv_t - \frac{1}{2}v_{xx} + \left(1 + \frac{\delta^2}{2} + \beta\delta\right) |v|^4 v + i \left[ (\beta + \delta) |v|^2 v_x + \left(\frac{\delta}{2} - \gamma\right) (|v|^2)_x v \right] = 0, \quad (8)$$

which will be the model of our focus hereafter. Obviously, the original system is now uncoupled\* and  $\psi_x = |v|^2$ . Here it should be noted that the model (8), having the form of an extended quintic NLS, differs from other extended versions of the NLS equation, relevant to water waves of finite depth (see, e.g., Refs. [40, 41], as well as discussion in Refs. [33, 34, 36]), which were used to predict bright and dark solitons on the surface of water [41]: indeed, the later models include also linear higher-order terms (e.g., third-order dispersion), while Eqs. (4) only incorporate higher-order nonlinear terms.

At this point, it is important to mention the following. In Ref. [32], as well as in the later works [33, 34], an equation similar to Eq. (8) was derived, namely:

$$iu_t - q_1 u_{xx} - q_2 |u|^4 u - i [q_3 |u|^2 u_x + q_4 (|u|^2)_x u] = 0, \quad (9)$$

where coefficients  $q_i \in \mathbb{R}_+$  ( $i \in \{1, \dots, 4\}$ ). Here, one should notice the difference in the signs of the coefficients – and, most notably, the one of the quintic term –

\*The reduction of Eq. (4) to Eq. (8) was also discussed in Ref. [32], but in a more involved fashion.

resulting in controversial results regarding the stability of the cw solution: in the framework of Eq. (4) it is modulationally stable (see below), while in the case of Eq. (9) it is subject to modulational instability [32–34]. This latter conclusion is also in agreement with Refs. [35, 36], which focused on the analysis of the canonical form of Eq. (9), corresponding to  $q_4 = 0$ . Nevertheless, as mentioned above, we will analyze Eq. (8) as a generic example of the more general model (3), which can support robust gray solitons.

Key to our analysis below is the fact that the cw solution of Eq. (8), namely:

$$v = \rho_0 \exp(-i\omega_0 t), \quad \omega_0 = - \left( 1 + \frac{\delta^2}{2} + \beta\delta \right) \rho_0^4, \quad (10)$$

where  $\rho_0$  is an arbitrary real constant, is modulationally stable (and thus gray solitons on top of this cw can be supported). This can easily be confirmed via a standard MI analysis (see, e.g., Ref. [2]), whereby the wavenumber  $k$  and frequency  $\omega$  of a small perturbation  $\propto \exp[i(kx - \omega t)]$  satisfy the following dispersion relation:

$$\omega = -\frac{1}{2}k \left[ \rho_0^2(-2\beta + 2\gamma - 3\delta) \pm \sqrt{k^2 + \alpha\rho_0^4} \right], \quad (11)$$

where

$$\alpha = 4\gamma^2 + 5\delta^2 + 4(2 + \beta\delta - 2\gamma\delta). \quad (12)$$

As long as  $\alpha > 0$ ,  $\omega \in \mathbb{R} \forall k \in \mathbb{R}$ , which means that the cw is modulationally stable. As we see below, the availability of coefficients  $\alpha_i$  ( $i \in \{1, 2, \dots, 6\}$ ) of Eq. (4) [31], which in turn provides the coefficients  $\beta$ ,  $\gamma$ , and  $\delta$  in Eq. (8), allows us to deduce that this is indeed the case: the parameter  $\alpha$  is always positive, and thus the cw solution (10) is modulationally stable  $\forall k \in \mathbb{R}$ .

## 2.2. REDUCTION TO THE KDV EQUATION AND SOLITON SOLUTIONS

Next, we apply the reductive perturbation method [38] to derive from Eq. (8) an effective KdV equation; the soliton solution of the latter, will be then used to derive approximate gray soliton solutions of Eq. (8). Notice that a similar approach has been used in the past in the context of nonlinear optics, where KdV-like gray solitons were obtained for NLS models perturbed by higher-order effects –see, e.g., Refs. [42, 43] where the analytical approach is also detailed. We start by introducing in Eq. (8) the Madelung transformation,

$$v(x, t) = \sqrt{\rho(x, t)} \exp[i\phi(x, t)], \quad (13)$$

where the real functions  $\rho$  and  $\phi$  denote, respectively, the density and phase of the unknown field  $v$ .

Then, considering small-amplitude slowly-varying modulations of the cw (10),

we look for solutions in the form of the following asymptotic expansions:

$$\rho = \rho_0 + \sum_{j=1}^{\infty} \epsilon^j \rho_j(X, T), \quad \phi = -\omega_0 t + \sum_{j=1}^{\infty} \epsilon^{j-1/2} \phi_j(X, T). \quad (14)$$

Here,  $0 < \epsilon \ll 1$  is a formal small parameter, and the unknown densities  $\rho_j$  and phases  $\phi_j$  are functions of the slow variables:

$$X = \epsilon^{1/2}(x - ct), \quad T = \epsilon^{3/2}t, \quad (15)$$

with  $c$  being the so-called ‘‘speed of sound’’ (to be determined), namely the speed of the linear waves propagating on top of the cw background. Notice that the specific form of the asymptotic expansions (14) as well as the choice of the slow variables (15) are such that dispersive and nonlinear effects come into play at the same order of approximation (see Ref. [38]).

At the lowest-order of the reductive perturbation technique, we arrive at a system of two linear equations. The compatibility condition of these equations is the algebraic equation:

$$c^2 - (2\beta - 2\gamma + 3\delta)\rho_0 c + (\delta^2 - 2\gamma\delta - 2\beta\gamma + \beta\delta + \beta^2 - 2)\rho_0^2 = 0, \quad (16)$$

from which we obtain the speed of sound:

$$c = c_{\pm} = \frac{1}{2}\rho_0 (2\beta - 2\gamma + 3\delta \pm \sqrt{\alpha}), \quad (17)$$

where  $\alpha$  is given in Eq. (12). We observe that the condition  $\alpha > 0$  ensuring that  $c \in \mathbb{R}$  is identical with the one concerning the stability of the cw solution. Nevertheless, as mentioned above,  $\alpha$  is positive, which dictates the existence of two speeds of sound, a ‘‘fast’’ and a ‘‘slow’’ one,  $c_+$  and  $c_-$ , respectively. In addition, at the same order of approximation:

$$\phi_{1X} = \Delta\rho_1, \quad \Delta = -\frac{(2\beta\delta + \delta^2 + 2)\rho_0}{c - (\beta + \delta)\rho_0}, \quad (18)$$

which connects the unknown phase  $\phi_1$  with the density  $\rho_1$ .

To the next order of approximation, we obtain two nonlinear equations. The compatibility conditions of the later is again the algebraic equation (16) and the KdV equation for the density  $\rho_1$ :

$$A\rho_{1T} + B\rho_1\rho_{1X} + \Gamma\rho_{1XXX} = 0, \quad (19)$$

where the coefficients  $A$ ,  $B$  and  $\Gamma$  are given by:

$$A = \frac{4\rho_0[2c + (2\gamma - 2\beta - 3\delta)\rho_0]}{c - (\beta + \delta)\rho_0}, \quad (20)$$

$$B = \frac{4\tilde{B}}{[c - (\beta + \delta)\rho_0]^2}, \quad (21)$$

$$\begin{aligned} \tilde{B} = & 2c^3 - c^2\rho_0(3\beta - 2\gamma + 4\delta) + 2c\rho_0^2(2 + 2\beta\delta + \delta^2) \\ & + \rho_0^3[\beta^3 + 2\gamma(2 - \beta^2) - \delta(6 + \delta^2) - \beta(4 + 3\delta^2)], \end{aligned} \quad (22)$$

$$\Gamma = -\frac{c - (\beta - 2\gamma + 2\delta)\rho_0}{(2 + 2\beta\delta + \delta^2)\rho_0}. \quad (23)$$

The soliton solution of the KdV, Eq. (19), reads:

$$\rho_1 = \frac{12\kappa^2\Gamma}{B} \operatorname{sech}^2 \left[ \kappa \left( X - \frac{4\kappa^2\Gamma}{A} T \right) - X_0 \right], \quad (24)$$

where  $\kappa$  is an arbitrary real constant of order  $O(1)$ , and  $X_0$  denotes the initial soliton position. Using Eq. (24), we can also determine the phase through Eq. (18), namely  $\phi_1 = \Delta \int \rho_1(X', T) dX'$ . To this end, using these expressions, we can write the relevant approximate solution of Eq. (8) in terms of the original variables as follows:

$$v(x, t) \approx \sqrt{\rho_0 + \frac{12\epsilon\kappa^2\Gamma}{B} \operatorname{sech}^2(\xi)} \exp \left[ -i\omega_0 t + \frac{12i\epsilon^{1/2}\kappa\Gamma\Delta}{B} \tanh(\xi) \right], \quad (25)$$

$$\xi = \epsilon^{1/2}\kappa \left[ x - c \left( 1 + \frac{4\epsilon\kappa^2\Gamma}{cA} \right) t - x_0 \right]. \quad (26)$$

As we will see below, here we have  $B\Gamma < 0$ ; this implies that the solution (25) is characterized by a  $\operatorname{sech}^2$ -shaped density dip, and a  $\tanh$ -shaped phase jump across the density minimum, thus having the form of a genuine gray soliton. At this point, it is important to point out that, since coefficients  $A$ ,  $B$ ,  $\Gamma$ , and  $\Delta$  are functions of  $c$ , which in turn takes two distinct values,  $c_{\pm}$  as per Eq. (17), the solution (25) describes simultaneously two different types of gray solitons, namely fast and slow ones, corresponding to  $c_+$  and  $c_-$ , respectively.

### 3. NUMERICAL RESULTS

Next, we compare our analytical findings with results of direct numerical simulations for Eq. (8). We start by considering the values of the parameters, as well as of the various coefficients involved in our analytical approach. First of all, we use the values of parameters  $\alpha_j$  appearing in Eq. (4) from Ref. [31], corresponding to the case  $kh = 1.363$ . These values, in turn, lead to the following ones for the coefficients

$\beta$ ,  $\gamma$ , and  $\delta$  appearing in Eqs. (5) and (8):

$$\beta = 1.764, \gamma = 1.147, \delta = 2.329.$$

Using the above, Eq. (12) dictates that parameter  $\alpha$  takes the value:  $\alpha = 62.558\rho_0^4 > 0$ . Thus, the cw background is indeed not subject to MI, and undergoes a stable evolution. This also suggests that there are two possible real solutions to Eq. (16), namely:

$$c_- = 0.156\rho_0 \quad \text{and} \quad c_+ = 8.065\rho_0,$$

leading to two possible gray solitons, as mentioned above. It is clear that one of them is almost stationary (the one corresponding to  $c_-$ ), while the second moves substantially faster (the one corresponding to  $c_+$ ). This allows us to respectively term these two solutions “slow” and “fast”.

Thanks to the nature of the KdV soliton (whereby amplitude, width and velocity are connected to each other through the parameter  $\kappa$ ), there exist also differences in the spatial profiles of the slow and fast gray solitons. To better illustrate these differences, in Fig. 1 we plot the two solutions at  $t = 0$ . We choose  $\rho_0 = 1$ ,  $\epsilon = 0.01$  and  $\kappa = 2$  for the slow solution while  $\kappa = 5$  for the fast, so that the relative amplitudes (dips) are comparable. As it is clearly seen, the slow solution is wider and deeper than the fast one, and it is thus expected to propagate slower than the other, following the KdV dynamics above.

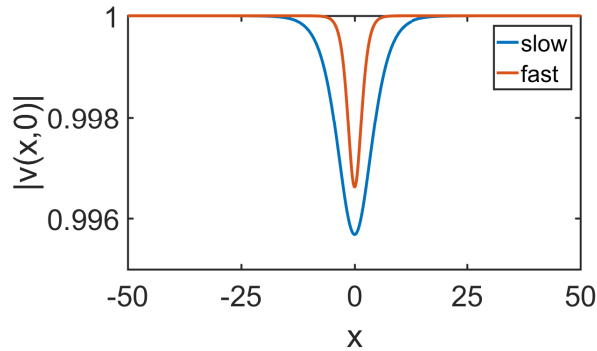


Fig. 1 – (Color online) The initial spatial profile of the fast (orange) and slow (blue) gray solitons. Evidently, the former is shallower and features a smaller width as compared to the latter. Parameter values are  $\rho_0 = 1$ , while  $\kappa = 2$  for the slow solution and  $\kappa = 5$  for the fast one.

We have also performed direct numerical simulations. In particular, employing a fourth order Runge-Kutta method, we have numerically integrated Eq. (8) and used initial conditions (at  $t = 0$ ) taken from Eqs. (25)-(26). In Fig. 2, we show the evolution of the fast and slow solitons, corresponding to the initial conditions of Fig. 1. The numerical results agree with our analytical findings: indeed, both solutions fol-



low the predicted KdV dynamics, preserving their shapes, and traveling with constant velocity  $C$ . In the simulations, we find that the latter is equal to:

$$C_{\text{fast}}^{(\text{num})} = 8 \quad \text{and} \quad C_{\text{slow}}^{(\text{num})} = 0.15,$$

for the fast and slow solitons, respectively. On the other hand, according to the analytical prediction, namely  $C = c [1 + 4\epsilon\kappa^2\Gamma/(cA)]$  (see Eq. (26)), the respective velocities are found to be:

$$C_{\text{fast}}^{(\text{an})} = 8.033 \quad \text{and} \quad C_{\text{slow}}^{(\text{an})} = 0.161.$$

Obviously, the agreement between numerical and analytical results is excellent. Nevertheless, it should be noticed that our analysis dictates the existence of a supersonic gray soliton, with  $C_{\text{slow}}^{(\text{an})} > c_-$ , which can not occur in the realm of defocusing NLS models [2, 3]. The fact that slow solitons were not only found to exist, but also to be robust in the simulations, implies that our analytical prediction for the solitons' velocities slightly overestimates  $C_{\text{slow}}$ .

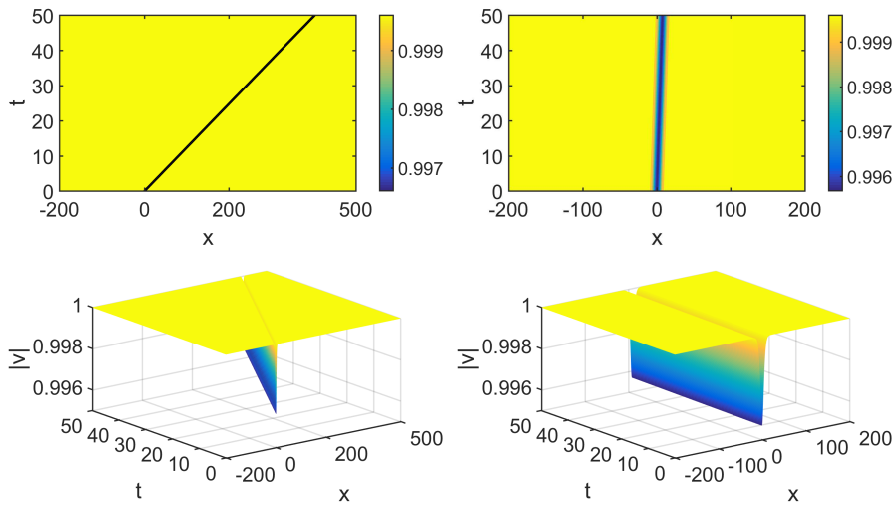


Fig. 2 – (Color online) Results of direct numerical simulations showing the evolution of the fast (left column) and slow (right column) gray solitons under the model Eq. (8). Shown are contour plots (top panels) and 3D plots (bottom panels) depicting the evolution of the modulus  $|v(x, t)|$ . Parameter values are, again,  $\rho_0 = 1$  and  $\kappa = 2$  for the slow solution while  $\kappa = 5$  for the fast one.

In any case, thanks to the significantly small value of the velocity  $c_-$  (and hence of  $C_{\text{slow}}$ ), the slow gray soliton is almost stationary (at the reference system traveling with the group velocity). This is a rather surprising result by itself for gray solitons, which are known to be fast traveling objects [2, 3].

#### 4. CONCLUSIONS

In conclusion, we have studied the existence, formation, and dynamics of gray solitons for an extended quintic NLS equation. The considered model was the one proposed in Ref. [31] for surface water waves, when the parameter  $kh$  takes the critical value  $kh = 1.363$ . This model possesses a stable cw solution, which contradicts later relevant results [32–36] dictating that the cw solution in this water wave problem (for  $kh = 1.363$ ) is unstable. However, the considered model can be viewed as a paradigmatic example of a general extended quintic NLS equation that can formally be obtained from any nonlinear dispersive system [37]; such a model, under certain conditions, can indeed support a stable cw solution, on top of which gray solitons can occur.

Our analysis revealed that this is the case. Indeed, the model under consideration was studied analytically by means of the reductive perturbation method, which led to an effective KdV equation. The soliton solution of the latter, was then used to derive two types of approximate gray soliton solutions of the original model: fast and slow ones.

Direct numerical simulations have shown that both types are particularly robust and evolve following closely the KdV dynamics. We have found that the velocity of the slow soliton is quite small, such that this type of soliton can be deemed to be almost stationary (in the reference frame moving with the group velocity), but with velocity exceeding the speed of sound thus deeming these objects unphysical. This is a particular feature of the extended quintic NLS equation under consideration, which, to the best of our knowledge, has no analogue in other contexts where gray solitons also appear – such as nonlinear optics [2] and Bose-Einstein condensates [3].

#### REFERENCES

1. V. E. Zakharov and A. B. Shabat, Zh. Eksp. Teor. Fiz. **64**, 1627 (1973) [Sov. Phys. JETP **37**, 823 (1973)]
2. Yu. S. Kivshar and B. Luther-Davies, Phys. Rep. **298**, 81 (1998).
3. D. J. Frantzeskakis, J. Phys. A: Math. Theor. **43**, 213001 (2010).
4. V. S. Bagnato, D. J. Frantzeskakis, P. G. Kevrekidis, B. A. Malomed, and D. Mihalache, Rom. Rep. Phys. **67**, 5 (2015).
5. P. G. Kevrekidis, D. J. Frantzeskakis, and R. Carretero-González, *The Defocusing Nonlinear Schrödinger Equation: From Dark Solitons and Vortices to Vortex Rings* (SIAM, Philadelphia, 2015).
6. D. Mihalache, Rom. Rep. Phys. **69**, 403 (2017).
7. B. Denardo, B. Galvin, A. Greenfield, A. Larraza, S. Putterman, and W. Wright, Phys. Rev. Lett. **68**, 1730 (1992).
8. P. Marquie, J. M. Bilbault, and M. Remoissenet, Phys. Rev. E **49**, 828 (1994).
9. M. Chen, M. A. Tsankov, J. M. Nash, and C. E. Patton, Phys. Rev. Lett. **70**, 1707 (1993).

10. R. Heidemann, S. Zhdanov, R. Sütterlin, H. M. Thomas, and G. E. Morfill, *Phys. Rev. Lett.* **102**, 135002 (2009).
11. A. Piccardi, A. Alberucci, N. Tabiryian, and G. Assanto, *Opt. Lett.* **36**, 1356 (2011).
12. I. V. Barashenkov and V. G. Makhankov, *Phys. Lett. A* **128**, 52 (1988).
13. L. J. Mulder and R. H. Enns, *IEEE J. Quantum Electron.* **25**, 2205 (1989).
14. J. Herrmann, *Opt. Commun.* **91**, 337 (1992).
15. F. G. Bass, V. V. Konotop, and S. A. Puzenko, *Phys. Rev. A* **46**, 4185 (1992).
16. P. F. Bedaque, E. Braaten, and H. W. Hammer, *Phys. Rev. Lett.* **85**, 908 (2000).
17. A. Gammal, T. Frederico, L. Tomio, and F. K. Abdullaev, *Phys. Lett. A* **267**, 305 (2000).
18. T. Chen and N. Pavlović, *J. Functional Analysis* **260**, 959 (2011).
19. A. Muryshev, G. V. Shlyapnikov, W. Ertmer, K. Sengstock, and M. Lewenstein, *Phys. Rev. Lett.* **89**, 110401 (2002).
20. L. Khaykovich and B. A. Malomed, *Phys. Rev. A* **74**, 023607 (2006).
21. E. B. Kolomeisky and J. P. Straley, *Phys. Rev. B* **46**, 11749 (1992).
22. E. B. Kolomeisky, T. J. Newman, J. P. Straley, and X. Qi, *Phys. Rev. Lett.* **85**, 1146 (2000).
23. D. J. Frantzeskakis, N. P. Proukakis, and P. G. Kevrekidis, *Phys. Rev. A* **70**, 015601 (2004).
24. A. Chabchoub, O. Kimmoun, H. Branger, N. Hoffmann, D. Proument, M. Onorato, and N. Akhmediev, *Phys. Rev. Lett.* **110**, 124101 (2013).
25. A. Chabchoub, O. Kimmoun, H. Branger, C. Kharif, N. Hoffmann, M. Onorato, and N. Akhmediev, *Phys. Rev. E* **89**, 011002(R) (2014).
26. M. J. Ablowitz, *Nonlinear Dispersive Waves: Asymptotic Analysis and Solitons* (Cambridge University Press, Cambridge, 2011).
27. T. B. Benjamin and J. E. Feir, *J. Fluid Mech.* **27**, 417 (1967).
28. H. C. Yuen and B. M. Lake, *Phys. Fluids* **18**, 956 (1975).
29. A. Chabchoub, N. P. Hoffmann, and N. Akhmediev, *Phys. Rev. Lett.* **106**, 204502 (2011).
30. S. Chen, F. Baronio, J. M. Soto-Crespo, P. Grelu, and D. Mihalache, *J. Phys. A: Math. Theor.* **50**, 463001 (2017).
31. R. S. Johnson, *Proc. R. Soc. Lond. A* **357**, 131 (1977).
32. T. Kakutani and K. Michihiro, *J. Phys. Soc. Jpn.* **52**, 4129 (1983).
33. Yu. V. Sedletsy, *J. Exp. Theor. Phys.* **97**, 180 (2003).
34. A. V. Slunyaev, *J. Exp. Theor. Phys.* **101**, 926 (2005).
35. D. S. Agafontsev, *JETP Lett.* **87**, 195 (2008).
36. R. H. J. Grimshaw and S. Y. Annenkov, *Stud. Appl. Math.* **126**, 409 (2011).
37. E. J. Parkes, *J. Phys. A: Math. Gen.* **20**, 2025 (1987).
38. A. Jeffrey and T. Kawahara, *Asymptotic Methods in Nonlinear Wave Theory* (Pitman, Boston, 1982).
39. E. Kengne and W. M. Liu, *Phys. Rev. E* **73**, 026603 (2006).
40. K. B. Dysthe, *Proc. R. Soc. Lond. A* **369**, 105 (1979).
41. I. S. Gandzha and Yu. V. Sedletsy, *Phys. Lett. A* **381**, 1784 (2017).
42. D. J. Frantzeskakis, *J. Phys. A: Math. Gen.* **29**, 3631 (1996).
43. D. J. Frantzeskakis, *J. Opt. Soc. Am. B* **14**, 2359 (1997).